# Frequency-Stable Robust Wireless Power Transfer Based on High-Order Pseudo-Hermitian Physics

Xianglin Hao,[*] Ke Yin,[*] Jianlong Zou,[†] Ruibin Wang, Yuangen Huang, Xikui Ma, and Tianyu Dong[‡]
*School of Electrical Engineering, Xi'an Jiaotong University, Xi'an 710049, China*

(Received 1 August 2022; accepted 17 January 2023; published 16 February 2023)

Nonradiative wireless power transfer (WPT) technology has made considerable progress with the application of the parity-time (PT) symmetry concept. In this Letter, we extend the standard second-order PT-symmetric Hamiltonian to a high-order symmetric tridiagonal pseudo-Hermitian Hamiltonian, relaxing the limitation of multisource/multiload systems based on non-Hermitian physics. We propose a three-mode pseudo-Hermitian dual-transmitter-single-receiver circuit and demonstrate that robust efficiency and stable frequency WPT can be attained despite the absence of PT symmetry. In addition, no active tuning is required when the coupling coefficient between the intermediate transmitter and the receiver is changed. The application of pseudo-Hermitian theory to classical circuit systems opens up an avenue for expanding the application of coupled multicoil systems.

DOI: 10.1103/PhysRevLett.130.077202

Wireless power transfer (WPT) shows exciting and promising applications in various fields where physical connections are not allowed. Driven by modern physical concepts [1–3] and the ever-increasing practical demand [4–8], the *so-called* magnetic resonance mechanism [9] for the nonradiative WPT technology has experienced rapid development in recent years. However, conventional WPT systems are not robust when source and load coils are dislocated or there is a relative motion, yielding a variation of mutual coupling. Towards this end, with the introduction of parity-time (PT)-symmetric systems [10–17], the non-Hermitian theory [18–20] has been applied to WPT technology to address the long-standing robustness issue. With a real frequency spectrum, PT-symmetric WPT systems can self-select the operating frequency that corresponds to the maximum efficiency and hence guarantee optimal power transfer over a wide range of transfer distances without any active tuning [12].

For a PT-symmetric WPT system, it requires gain elements covering the entire operating frequency range [12,13,21], which may increase the complexity and cost since the frequency variation range may be large when the natural resonant frequency of the coil is high. In addition, the PT-symmetric phase requires the coupling coefficient $k$ to be greater than the normalized gain-loss parameter $\gamma$ which is typically determined by the resistance of the gain-loss resonators [22,23]; thus, the efficient working range of the system is usually limited by the resistance. Although high-order PT-symmetric systems are expected to achieve robust WPT with locked frequencies [21,24], the coupling coefficients between adjacent resonators must be equal to support the PT-symmetric phase. As a consequence, it generally requires precise mechanical control of the system, which can lead to a substantial increase in complexity and cost.

For non-Hermitian systems, a real spectrum could exist not only in a PT-symmetric system but also in the *so-called* pseudo-Hermitian one whose Hamiltonian satisfies $\boldsymbol{\mu} \boldsymbol{H} \boldsymbol{\mu}^{-1} = \boldsymbol{H}^{\dagger}$, where $\boldsymbol{\mu}$ is a Hermitian invertible operator [25–27] and "†" denotes the Hermitian conjugation, showing a more general class of Hamiltonians with real eigenvalues [25,26]. In this Letter, the conventional PT-symmetric WPT is extended to construct a multicoil WPT system based on pseudo-Hermitian physics. As a prototype, we report a dual-transmitter-single-receiver system that incorporates nonlinear saturable gain elements into the source for WPT applications. It is shown that, even though the system is not PT symmetric, it still has real eigenfrequencies for varying coupling coefficients, and one of the eigenfrequencies does not change with respect to the coupling coefficient in the strong coupling region. Thus, we can achieve frequency-stable, high-efficiency power transfer in the strong coupling region by utilizing the saturation characteristic of nonlinear gain elements, while the frequency only changes slightly in the weak coupling region.

We start by constructing a class of higher-order WPT systems whose Hamiltonians are tridiagonal matrices from the standard second order PT-symmetric WPT system [12,14–16], as shown in Fig. 1(a). Within the coupled mode theory [28], the time evolution of the amplitudes of the transmitter and receiver resonator for the standard PT-symmetric dimer, denoted by $\mathbf{a} = [a_1, a_2]^T$, is governed by [11–13,22]

$$i \frac{d\mathbf{a}}{dt} = \boldsymbol{H}_{\mathrm{std}} \mathbf{a}, \tag{1}$$

 

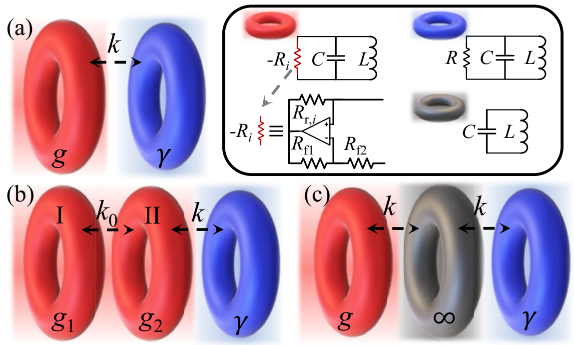


FIG. 1. Schematics of (a) a standard PT-symmetric electronic dimer, (b) a three-mode pseudo-Hermitian system consisting of two gain (red) units and one loss (blue) unit, and (c) a conventional three-coil PT-symmetric system consisting of balanced gain and loss, as well as neutral (gray) electronic molecules. Here, $k$ or $k_0$ denotes the coupling coefficients between neighboring resonators; and the mutual coupling between the nonadjacent resonators [e.g., the transmitter I and receiver in (b)] is assumed to be negligible.

where

$$\boldsymbol{H}_{\rm std} = \begin{pmatrix} H_{11} & H_{12} \\ H_{21} & H_{22} \end{pmatrix} = \omega_0 \begin{pmatrix} 1+i\gamma & \kappa \\ \kappa & 1-i\gamma \end{pmatrix} \quad (2)$$

is the Hamiltonian. Here, $H_{11} = H_{22}^* = \omega_0(1+i\gamma)$ with $\gamma$ denoting gain (or loss) and "*" denoting conjugation, and $H_{12} = H_{21} = \omega_0\kappa$ with $\kappa$ denoting the mutual coupling between the resonators whose eigenfrequency are $\omega_0$. If the element $H_{11}$ or $H_{22}$ is replaced by a second-order block matrix of the same form as $\boldsymbol{H}_{\rm std}$ *per se*, and the mutual coupling is only considered for neighboring resonators, i.e., $H_{21} = H_{12}^T = [\kappa_{13}, \kappa_{23}]$, where $\kappa_{13} = 0$, we can form a three-mode system, which can be a two-transmitter-one-receiver [see Fig. 1(b)], a one-transmitter-two-receiver, or a transmitter-repeater-receiver [see Fig. 1(c)] system. In a similar manner, chainlike high-order systems can be constructed whose Hamiltonians are symmetric tridiagonal if the mutual couplings for nonadjacent resonators are neglected. Since each resonator can be gainy, lossy, or lossless, the corresponding Hamiltonian is a non-Hermitian symmetric matrix in general, whose diagonal elements can be complex and the off-diagonal elements are all real. For high-order systems, such a Hamiltonian corresponds to a multiple-transmitter, multiple-receiver WPT system. In addition, a symmetric tridiagonal Hamiltonian can be PT symmetric or pseudo-Hermitian, functioning in WPT applications.

We focus on the Hamiltonian, which describes a dual-transmitter-single-receiver WPT system, as shown in Fig. 1(b), i.e.,

$$\boldsymbol{H}_{\rm pse} = \frac{\omega_0}{2} \begin{pmatrix} 2+ig_1 & k_0 & 0 \\ k_0 & 2+ig_2 & k \\ 0 & k & 2-i\gamma \end{pmatrix}, \quad (3)$$

which has been proved to be a pseudo-Hermitian Hamiltonian under certain conditions [29]. Here, $g_1$ and $g_2$ describe the strength of the gain in the transmitter resonators I and II, respectively; $\gamma$ is the loss constant of the receiver resonator; $k_0$ denotes the coupling coefficient between the two gain resonators; and $k$ denotes the coupling coefficient between the transmitter resonator II and the receiver resonator. The natural resonant frequencies of all the resonators are tuned to be $\omega_0$. Such a Hamiltonian (3) can form a PT-symmetric system [see Fig. 1(c)] when $g_1 = \gamma$, $g_2 = 0$, and $k_0 = k$ [21,24]. Moreover, even if it is not PT symmetric, the Hamiltonian (3) can still have real eigenvalues [30]. By solving the characteristic equation $\det(\omega\mathbf{I} - \boldsymbol{H}_{\rm pse}) = 0$ (where $\mathbf{I}$ denotes an identity matrix), one arrives at

$$\Delta\tilde{\omega}\left[\Delta\tilde{\omega}^2 + \frac{1}{4}(\gamma g_1 + \gamma g_2 - g_1 g_2 - k^2 - k_0^2)\right] + \frac{i}{2}\left[(g_1 + g_2 - \gamma)\Delta\tilde{\omega}^2 + \frac{1}{4}(g_1 g_2 \gamma + k_0^2\gamma - k^2 g_1)\right] = 0, \quad (4)$$

where $\Delta\tilde{\omega} = \tilde{\omega} - 1$ with $\tilde{\omega} = \omega/\omega_0$ being the normalized angular frequency. Instead of forcing the imaginary part of (4) to be zero [12], we can combine the like terms, which yields $\Delta\tilde{\omega}[\Delta\tilde{\omega} \pm \sqrt{4\tilde{\kappa} - c^2}/4 - ic/4] = 0$ where $\tilde{\kappa} = k_0^2 + k^2 + g_1 g_2 - \gamma(g_1 + g_2)$ and $c = g_1 + g_2 - \gamma$. Thus, in the strong coupling region when $k \geq \gamma$, three modes could exist, whose eigenfrequencies read as

$$\omega_1 = \omega_0, \quad (5a)$$

$$\omega_{2,3} = \omega_0(1 \pm \sqrt{4\tilde{\kappa} - c^2}/4 - ic/4). \quad (5b)$$

According to (4), provided that the criterion

$$(g_1 g_2 + k_0^2)\gamma = k^2 g_1 \quad (6)$$

is satisfied, the real mode $\omega = \omega_1$ could exist, no matter if the modes $\omega_{2,3}$ are complex or real, which provides great design freedom. Note that the system can support seven modes in total when taking into account the frequency-dependent nonlinear gain (see Supplemental Material [31] for a detailed analysis). Here, we only show the modes corresponding to the frequency-independent gain, not all possible modes. In the weak coupling region regime when $k < \gamma$, only two real-eigenvalue states exist and the corresponding eigenfrequencies read as

$$\omega_{2,3} = \omega_0(1 \pm \sqrt{\tilde{\kappa}}/2), \quad (7)$$

and $\omega_1 = \omega_0 - ic/2$ denoting the unstable states; while we have the criterion

$$(g_1 g_2 \gamma + k_0^2 \gamma - k^2 g_1) c^{-1} = -\tilde{\kappa} \quad (8)$$

to support the stable-frequency mode for the weak coupling regime. We shall point out that one can control the coupling regions by changing $\gamma$ and $k_0$ so that the phase transition may be independent of load, showing a fascinating realm in WPT applications. In a similar manner, one can handle the Hamiltonian (3) of a single-transmitter dual-receiver system by the time-reversal transformation [19,32]. Furthermore, within the proposed method, one may be able to analyze the stable frequency mode of the pseudo-Hermitian extensions on anti-parity-time symmetry systems [33–35] when the coupling coefficients are pure imaginary, and even systems with complex coupling coefficients [27,36].

We first consider the case when the strong coupling region supports three real modes when $c = 0$. To design a pseudo-Hermitian WPT system with the known load denoted by $\gamma$, one can determine the two gain coefficients, $g_1$ and $g_2$, of the system according to the coupling coefficients, $k$ and $k_0$, as implicated by (6) or (8). In the strong coupling region when $k \geq \gamma$, the steady-state gains $g_1$ and $g_2$ can be obtained by solving $c = 0$ and (6) as $g_{1,2} = [\gamma^2 \mp k^2 \pm \sqrt{(\gamma^2 - k^2)^2 + 4\gamma^2 k_0^2}]/(2\gamma)$. It is evident that the sum of gain coefficients of the system is always equal to the loss coefficient $\gamma$, i.e., $g_1 + g_2 = \gamma$. When $k \gg k_0 = \gamma$, the gain coefficient $g_2$ dominates as $g_2 \gg g_1$. As $k$ is decreased, $g_2$ is decreased while $g_1$ is increased; when $g_1 = \gamma$ and $g_2 = 0$, the system is in the PT-symmetric state. In the weak coupling region when $k < \gamma$, $g_1$ and $g_2$ are related according to (8). For a given value of $g_1$ or $g_2$, one can determine the other gain; for instance, when $g_2 = 0$ for the intermediate resonator II in the weak coupling region, one obtain the gain for the source resonator I reads as $g_1 = [\gamma^2 + k_0^2 - \sqrt{(\gamma^2 + k_0^2)^2 - 4\gamma^2 k^2}]/(2\gamma)$, which is rapidly decreased to zero as $k$ is decreased.

In this Letter, we focus on the scenario when $k_0 = \gamma$ to achieve the same phase transition point as the standard PT-symmetric system for comparison. As shown in Figs. 2(a) and 2(b), the proposed three-mode pseudo-Hermitian system has a unique frequency characteristic with an open band gap, while the conventional PT-symmetric systems have an exceptional point in the transition from the strong coupling region to the weak coupling region [see in Figs. 2(c)–2(f)]. Such a unique frequency characteristic reflects the asymmetry of the pseudo-Hermitian system, which can be tuned by changing the ratio of coupling coefficients, i.e., $k_0/k$. In addition, the system has a steady-state frequency that does not vary with $k$ in the strong coupling region when $k \geq \gamma$, while its steady-state frequency can be designed in a narrow frequency range in the weak coupling region when $k < \gamma$. Therefore, such a three-coil pseudo-Hermitian system can be used to realize WPT with an almost stable operating frequency, even in the weak coupling regime. Note that the steady-state frequency will inevitably undergo discontinuous jumps when the system whose operating frequency is set to $\omega_1$ in the strong coupling region enters into the weak coupling region through the phase transition point, showing a possibility to further enhance the sensitivity in wireless sensing applications [23,37,38].

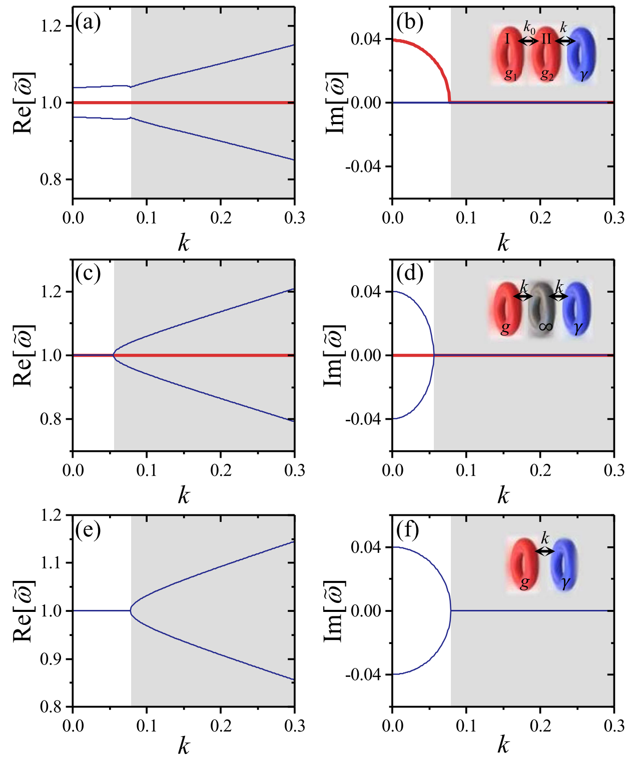


FIG. 2. Evolution of the real (left panel) and imaginary (right panel) parts of the normalized eigenfrequencies $\tilde{\omega} = \omega/\omega_0$ as a function of the coupling coefficient $k$ for various non-Hermitian systems, i.e., (a),(b) three-mode pseudo-Hermitian system, (c),(d) three-coil PT-symmetric system, and (e),(f) standard PT-symmetric system. For all three systems, the loss parameter reads $\gamma = 0.078$. Here, the blue curves denote the conjugate solution of $\omega$, while the red curves denote the additional solution of $\omega_1$ for three-mode systems. The ideal three-coil PT-symmetric WPT system always works in the state [red line in (c),(d)] where the frequency does not change with respect to the coupling coefficient $k$. The strong coupling regions are denoted by shading.

As shown in Fig. 2(a), the eigenfrequency $\omega_1 = \omega_0$ is locked to the natural frequency of the $LC$ tank, which is independent of the coupling coefficient $k$ in the strong coupling region. For the eigenstates denoted by $\omega_{2,3}$, only a small derivation of $\pm\sqrt{\tilde{\kappa}}/2$ of the eigenfrequency is presented, both for the strong and weak coupling regime. Therefore, high-efficiency power transfer always appears around $\omega_0$. Moreover, the pseudo-Hermitian system relaxes the limitation that the coupling coefficients $k_0$ and $k$ must be identical for the conventional three-coil PT-symmetric system. Compared with the standard second-order PT-symmetric system, whose eigenfrequencies are sensitive to the change of $k$ and $\gamma$ [see Figs. 2(e) and 2(f)] in the strong coupling region, the proposed pseudo-Hermitian

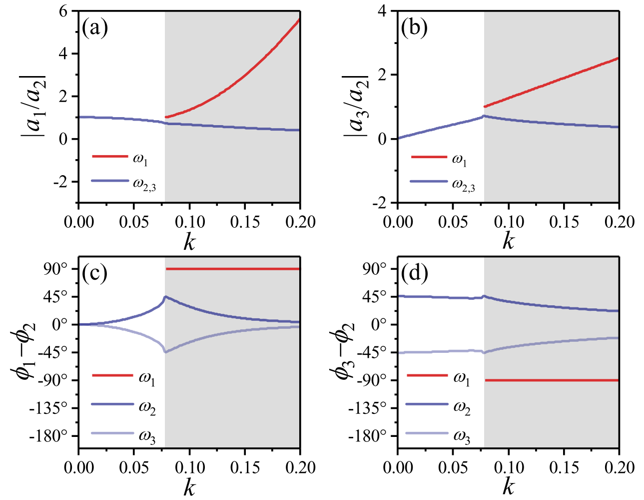


FIG. 3. Evolution of the amplitude ratios (a) $|a_1/a_2|$ and (b) $|a_3/a_2|$, and the phase differences $\phi_1-\phi_2$ and (d) $\phi_3-\phi_2$ as functions of the coupling coefficient $k$ at steady state. In all the subfigures, the gray vertical reference line indicates $k=\gamma=0.078$.

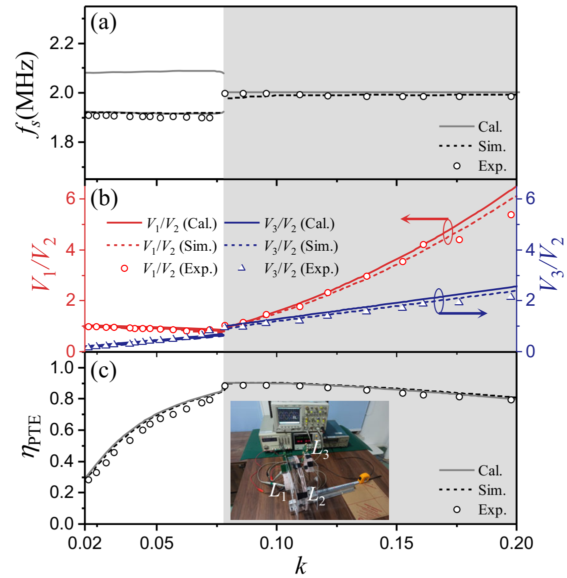


FIG. 4. (a) Steady-state frequency $f_s$, (b) voltage ratios $V_1/V_2$ (red for the left $y$ axis) and $V_3/V_2$ (blue for the right $y$ axis), and (c) power transmission efficiency $\eta_{\mathrm{PTE}}$ as functions of the coupling coefficient $k$. Theoretical (cal.), simulated (sim.) and experimental (exp.) results are illustrated by solid curves, dashed curves, and hollow markers, respectively. The shading regions indicate $k\geq\gamma=0.078$. The inset of (c) shows a photo of our experiment setup.

system is more friendly when designing the gain elements, which is expected to achieve a higher power transmission by combining the two transmitters.

The proposed three-mode pseudo-Hermitian system has unique power transfer properties. In the strong coupling region when $k\geq\gamma$, the ratios of the resonators' amplitudes, respectively, reads $a_1/a_2=ik_0/g_1$ and $a_3/a_2=-ik/\gamma$ for the mode $\omega_1=\omega_0$; while in the weak coupling region when $k<\gamma$, they are $a_1/a_2=k_0/(-ig_1\pm\sqrt{\tilde{\kappa}+\gamma g_2})$ and $a_3/a_2=k/(i\gamma\pm\sqrt{\tilde{\kappa}+\gamma g_2})$, respectively. Figures 3(a) and 3(b) plot the amplitude ratios as functions of the coupling coefficients. When the steady-state frequency switches from $\omega_1$ ($k\geq\gamma$ in the strong coupling region) to $\omega_{2,3}$ ($k<\gamma$ in the weak coupling region) at the phase transition point $k_0=0.078$, a small but abrupt change in the amplitude ratio appears. Although it would lead to a small, abrupt efficiency change around the transition point, it does not affect the stability of the system. In the strong coupling region, the range of the amplitude ratio for the steady state denoted by $\omega_1$ is greater than that for the state denoted by $\omega_2$ or $\omega_3$. Such varying amplitude ratios demonstrate the possibility of implementing a transformer in WPT systems, which may be beneficial for the applications of extracting energy from high-voltage power transmission lines. Moreover, as illustrated in Figs. 3(c) and 3(d), when the system frequency is locked at $\omega_1=\omega_0$ in the strong coupling region, the phase differences between the resonators are constant, which is more friendly for monitoring the system operation state. As for the power transmission efficiency, while it may not be constant for the proposed system due to the fluctuating amplitude ratio with regard to the coupling coefficient $k$, it is essentially stable in the strong coupling region if the quality factors of the resonators are sufficiently high [21,31,39].

The implementation of gain elements in non-Hermitian systems is crucial for WPT applications. According to the criterion (6), the gain strengths $g$'s are related to the coupling coefficient $k$. To avoid active tuning of gain when $k$ changes, nonlinear gain elements consisting of an operational amplifier (op-amp) can be adopted [11,12,37], as illustrated in the inset of Fig. 1. Because of the nonlinearity and saturation behaviors of op-amps [12], the actual gain $g_n(|a_n|)$ ($n=1,\ 2$) of the transmitters depends on the mode amplitude $|a_n|$, which will decrease as $|a_n|$ is increased beyond the threshold. If the op-amps are configured to saturation with the initial unsaturated gains $g_{n,i}$ being respectively greater than or equal to the corresponding steady-state desired gains, i.e., $g_{n,i}\geq g_n$, the system will eventually go into the stable oscillating state [31].

We have verified the theory via circuit simulations and experiments of the two-transmitter-one-receiver system [31]. All the coils are tuned to be resonant at 2 MHz, and the initial gains are $g_{1i}=0.113$ and $g_{2i}=0.005$, respectively. As a result, only a single steady state $\omega_1=\omega_0$ exhibits in the strong coupling region since $\omega_{2,3}$ are complex. Figure 4 shows the steady-state operating frequency $f_s$, resonators' voltage ratios, and the power transmission efficiency (PTE) $\eta_{\mathrm{PTE}}$ with respect to the coupling coefficient $k$. The experimental results show good agreement with the simulated and theoretical results. As shown in Fig. 4(a), the operating frequency is kept at about 2 MHz as the coupling coefficient $k$ varies from 0.078 to approximately 0.2 in the strong coupling region, without any tuning of the circuit. In the strong coupling region, the system has almost stable transmission efficiency, as illustrated in Fig. 4(b). In addition, the efficiency would slightly drop due to the overcoupling as $k$ increased. Both the simulation and experimental results demonstrate the transition of the steady-state frequency at around $k = \gamma$, which implicates that the frequency band gap exhibits in the system. Since the amplitude ratios of the resonator are discontinuous at the transition point $k = \gamma$, a slight abrupt change of the transmission efficiency appears. Such a transition would only introduce slight changes in frequency and efficiency in the weak coupling region, which would not affect the stable operation of the WPT system.

By optimizing the loss constant $\gamma$ and/or the coupling coefficient $k_0$, one may further improve the efficiency and the robustness of the proposed system. Moreover, if aiming to design a practical system with a single transmitter, no intermediate gain element is required [31]. For a lossy relay coil, assuming the additional gain $g_2 = -\gamma_{s2}$, we can also achieve a frequency-stable three-coil WPT system provided that the gain of the transmitter reads $g_1 = k_0^2\gamma/(k^2 + \gamma_{s2}\gamma)$. Given that the amplitude ratios of the system are fixed, highly efficient voltage-adjustable switch-mode amplifiers could be designed for a practical system to achieve constant power output. In addition, based on the concept of generalized PT symmetry [23,40], the inductance of the proposed system can be further optimized to facilitate coil design. For practical systems, high-efficiency switch-mode amplifiers [13–15] can be used as gain elements to achieve a high overall system efficiency.

In summary, we have reported a three-mode pseudo-Hermitian system constituting nonlinear gain-saturating elements for robust dynamic wireless power transfer operated at an almost fixed frequency without any active tuning. The proposed system always has real eigenfrequencies, even though it is not PT symmetric. The system also exhibits varying amplitude ratios, promising multifunctional platforms for transformers and wireless power transfer. Our work reveals that the multimode electronic circuit concept based on non-Hermitian physics with nonlinear gain holds promising for efficient dynamic wireless power transfer without active tuning. Meanwhile, our theory is expected to be applicable to handle multicoil WPT systems when relay coils are lossy, while the existing PT-symmetric systems generally fail [41,42]. Although the dual-transmitter-single-receiver topology is considered here, one may readily apply the time-reversal transformation [19] to handle the single-transmitter-dual-receiver circuit [43]. Moreover, our research may open a door to the investigation of the multiple-transmitter-one-receiver, one-transmitter-multiple-receiver, and multiple-transmitter-multiple-receiver WPT systems by virtue of pseudo-Hermitian physics.

The authors acknowledge support from the National Natural Science Foundation of China (NSFC) with Grant No. 51977165.

*These authors contributed equally to this work.
†superzou@mail.xjtu.edu.cn
‡Corresponding author.
tydong@mail.xjtu.edu.cn

[1] A. Krasnok, D. G. Baranov, A. Generalov, S. Li, and A. Alù, Coherently Enhanced Wireless Power Transfer, Phys. Rev. Lett. **120**, 143901 (2018).
[2] M. Song, P. Jayathurathnage, E. Zanganeh, M. Krasikova, P. Smirnov, P. Belov, P. Kapitanova, C. Simovski, S. Tretyakov, and A. Krasnok, Wireless power transfer based on novel physical concepts, Nat. Electron. **4**, 707 (2021).
[3] C. Zeng, Z. Guo, K. Zhu, C. Fan, G. Li, J. Jiang, Y. Li, H. Jiang, Y. Yang, Y. Sun, and H. Chen, Efficient and stable wireless power transfer based on the non-Hermitian physics, Chin. Phys. B **31**, 010307 (2022).
[4] X. Lu, D. Niyato, P. Wang, D. I. Kim, and Z. Han, Wireless charger networking for mobile devices: Fundamentals, standards, and applications, IEEE Wirel. Commun. **22**, 126 (2015).
[5] H. Dai, Y. Liu, G. Chen, X. Wu, T. He, A. X. Liu, and H. Ma, Safe charging for wireless power transfer, IEEE/ACM Trans. Netw. **25**, 3531 (2017).
[6] T. Kan, F. Lu, T.-D. Nguyen, P. P. Mercier, and C. C. Mi, Integrated coil design for EV wireless charging systems using LCC compensation topology, IEEE Trans. Power Electron. **33**, 9231 (2018).
[7] S. Zhang, Z. Qian, J. Wu, F. Kong, and S. Lu, Wireless charger placement and power allocation for maximizing charging quality, IEEE Trans. Mob. Comput. **17**, 1483 (2018).
[8] L. Li, X. Zhang, C. Song, and Y. Huang, Progress, challenges, and perspective on metasurfaces for ambient radio frequency energy harvesting, Appl. Phys. Lett. **116**, 060501 (2020).
[9] A. Kurs, A. Karalis, R. Moffatt, J. D. Joannopoulos, P. Fisher, and M. Soljačić, Wireless power transfer via strongly coupled magnetic resonances, Science **317**, 83 (2007).
[10] C. M. Bender and S. Boettcher, Real Spectra in Non-Hermitian Hamiltonians having PT Symmetry, Phys. Rev. Lett. **80**, 5243 (1998).
[11] J. Schindler, A. Li, M. C. Zheng, F. M. Ellis, and T. Kottos, Experimental study of active LRC circuits with PT symmetries, Phys. Rev. A **84**, 040101(R) (2011).
[12] S. Assawaworrarit, X. Yu, and S. Fan, Robust wireless power transfer using a nonlinear parity-time-symmetric circuit, Nature (London) **546**, 387 (2017).
[13] S. Assawaworrarit and S. Fan, Robust and efficient wireless power transfer using a switch-mode implementation of a nonlinear parity-time symmetric circuit, Nat. Electron. **3**, 273 (2020).

[14] J. Zhou, B. Zhang, W. Xiao, D. Qiu, and Y. Chen, Nonlinear parity-time-symmetric model for constant efficiency wireless power transfer: Application to a drone-in-flight wireless charging platform, IEEE Transactions on Industrial Electronics **66**, 4097 (2019).

[15] L. Wu, B. Zhang, and Y. Jiang, Position-independent CC/CV wireless EV charging system without dual-side communication and DC-DC converter, IEEE Transactions on Industrial Electronics **69**, 7930 (2022).

[16] Z. Hua, K. T. Chau, W. Liu, and X. Tian, Pulse frequency modulation for parity-time-symmetric wireless power transfer system, IEEE Trans. Magn. **58**, 8002005 (2022).

[17] X. Yang, J. Li, Y. Ding, M. Xu, X.-F. Zhu, and J. Zhu, Observation of Transient Parity-Time Symmetry in Electronic Systems, Phys. Rev. Lett. **128**, 065701 (2022).

[18] Y. Ashida, Z. Gong, and M. Ueda, Non-Hermitian physics, Adv. Phys. **69**, 249 (2020).

[19] K. Kawabata, K. Shiozaki, M. Ueda, and M. Sato, Symmetry and Topology in Non-Hermitian Physics, Phys. Rev. X **9**, 041015 (2019).

[20] R. El-Ganainy, K. G. Makris, M. Khajavikhan, Z. H. Musslimani, S. Rotter, and D. N. Christodoulides, Non-Hermitian physics and PT symmetry, Nat. Phys. **14**, 11 (2018).

[21] M. Sakhdari, M. Hajizadegan, and P.-Y. Chen, Robust extended-range wireless power transfer using a higher-order PT-symmetric platform, Phys. Rev. Res. **2**, 013152 (2020).

[22] J. Schindler, Z. Lin, J. Lee, H. Ramezani, F. M. Ellis, and T. Kottos, PT-symmetric electronics, J. Phys. A **45**, 444029 (2012).

[23] P.-Y. Chen, M. Sakhdari, M. Hajizadegan, Q. Cui, M. M.-C. Cheng, R. El-Ganainy, and A. Alù, Generalized parity-time symmetry condition for enhanced sensor telemetry, Nat. Electron. **1**, 297 (2018).

[24] C. Zeng, Y. Sun, G. Li, Y. Li, H. Jiang, Y. Yang, and H. Chen, High-Order Parity-Time Symmetric Model for Stable Three-Coil Wireless Power Transfer, Phys. Rev. Appl. **13**, 034054 (2020).

[25] A. Mostafazadeh, Pseudo-Hermiticity versus PT symmetry: The necessary condition for the reality of the spectrum of a non-Hermitian Hamiltonian, J. Math. Phys. (N.Y.) **43**, 205 (2002).

[26] A. Mostafazadeh, Pseudo-Hermiticity versus PT-symmetry III: Equivalence of pseudo-Hermiticity and the presence of antilinear symmetries, J. Math. Phys. (N.Y.) **43**, 3944 (2002).

[27] V. L. Grigoryan and K. Xia, Pseudo-Hermitian magnon-polariton system with a three-dimensional exceptional surface, Phys. Rev. B **106**, 014404 (2022).

[28] H. A. Haus and W. Huang, Coupled-mode theory, Proc. IEEE **79**, 1505 (1991).

[29] W. Xiong, Z. Li, Y. Song, J. Chen, G.-Q. Zhang, and M. Wang, Higher-order exceptional point in a pseudo-Hermitian cavity optomechanical system, Phys. Rev. A **104**, 063508 (2021).

[30] Z. Li, X. Li, and X. Zhong, High-order exceptional point in a nanofiber cavity quantum electrodynamics system, arXiv:2201.03768.

[31] See Supplement Material at http://link.aps.org/supplemental/10.1103/PhysRevLett.130.077202 for implementation of gain elements and detailed information on the simulation and experimental setup.

[32] R. G. Sachs, *The Physics of Time Reversal* (University of Chicago Press, Chicago 1987).

[33] Y. Choi, C. Hahn, J. W. Yoon, and S. H. Song, Observation of an anti-PT-symmetric exceptional point and energy-difference conserving dynamics in electrical circuit resonators, Nat. Commun. **9**, 2182 (2018).

[34] X.-W. Luo, C. Zhang, and S. Du, Quantum Squeezing and Sensing with Pseudo-Anti-Parity-Time Symmetry, Phys. Rev. Lett. **128**, 173602 (2022).

[35] M. Kim, Y. Yang, Y. Gui, and C.-M. Hu, Visualization of synchronization zone on the Bloch sphere through an anti-PT-symmetric electrical circuit, AIP Adv. **12**, 035217 (2022).

[36] G. Arwas, S. Gadasi, I. Gershenzon, A. Friesem, N. Davidson, and O. Raz, Anyonic-parity-time symmetry in complex-coupled lasers, Sci. Adv. **8**, eabm7454 (2022).

[37] K. Yin, Y. Huang, C. Ma, X. Hao, X. Gao, X. Ma, and T. Dong, Wireless real-time capacitance readout based on perturbed nonlinear parity-time symmetry, Appl. Phys. Lett. **120**, 194101 (2022).

[38] M. Yang, Z. Ye, M. Farhat, and P.-Y. Chen, Ultrarobust wireless interrogation for sensors and transducers: A non-Hermitian telemetry technique, IEEE Trans. Instrum. Meas. **70**, 1504709 (2021).

[39] D.-W. Seo, Comparative analysis of two-and three-coil WPT systems based on transmission efficiency, IEEE Access **7**, 151962 (2019).

[40] Z. Ye, M. Farhat, and P.-Y. Chen, Tunability and switching of Fano and Lorentz resonances in PTX-symmetric electronic systems, Appl. Phys. Lett. **117**, 031101 (2020).

[41] H. Kim, S. Yoo, H. Joo, J. Lee, D. An, S. Nam, H. Han, D.-H. Kim, and S. Kim, Wide-range robust wireless power transfer using heterogeneously coupled and flippable neutrals in parity-time symmetry, Sci. Adv. **8**, eabo4610 (2022).

[42] Y. Qu, B. Zhang, W. Gu, and X. Shu, Wireless power transfer system with high-order compensation network based on parity-time-symmetric principle and relay coil, IEEE Trans. Power Electron. **38**, 1314 (2022).

[43] F. Mohseni, A. Nikzamir, H. Cao, and F. Capolino, One-transmitter multiple-receiver wireless power transfer system using an exceptional point of degeneracy, arXiv:2204.10928.